output and the exact derivative of the bandlimited signal used in this simulation. Similar to the previous examples of Figs. 5 and 8, the interpolation error may be controlled by the tradeoff between computing time and accuracy. In this case, only the first six rows of the matrix C_u were retained for an overall error of -75 dB.

IV. Conclusions

The design [3] of digital filters whose output equations may, optionally, produce interpolated values at predetermined times is extended, in this correspondence, to those cases that require real-time computation of the interpolation time instants. In all its variants, the method provides the accurate digital replica of an analog prototype, with the exact mapping of the transfer function poles mentioned above, in Section II-C. Due to this accuracy, the proposed design preserves the advantages of optimal filter design methods. For example, an optimal FIR filter may be approximated with an analog filter, which will generate the interpolating digital filter operators. This is illustrated by the linear-phase digital filters of Tables II and III and Figs. 3–5.

The main contribution of this correspondence is the simple tradeoff between the accuracy and number of multiplications per interpolation point resulting from the properties of the operator $C_{T1,\,T2}$. Moreover, in the frequent case of digital filters followed by sampling rate conversion, a unique *interpolating digital filter with linear phase* was shown to eliminate the additional “interpolation filters” required by conventional approaches. A second class of applications is provided by the simulation software for performance evaluation of communication systems [2]. Thus, analog filters, together with the interpolated output, are accurately and efficiently modeled. In addition, the flexibility of the proposed design methods allows for simple simulation of multirate processes that are frequently encountered in the practice of simulation. Finally, the accuracy of the proposed digital filters can be used to advantage in the design of equipment for performance measurement.

References

[1] M. E. Frerking, *Digital Signal Processing in Communication Systems.* New York: Van Nostrand Reinhold, 1994.

[2] M. C. Jeruchim, P. Balaban, and K. S. Shanmugan, *Simulation of Communication Systems.* New York: Plenum, 1992.

[3] G. Braileanu, “Extended-window interpolation applied to digital filter design,” *IEEE Trans. Signal Processing,* vol. 44, pp. 457–472, Mar. 1996.

[4] L. W. Couch, II, *Digital Communications Systems.* New York: Macmillan, 1990.

[5] R. E. Crochiere, and L. R. Rabiner, *Multirate Digital Signal Processing.* Englewood Cliffs, NJ: Prentice-Hall, 1983.

[6] R. E. Blahut, *Digital Transmission of Information.* New York: Addison-Wesley, 1990.

[7] F. J. Harris, “On the use of windows for harmonic analysis with the discrete Fourier transform,” *Proc. IEEE,* vol. 66, pp. 51–83, Jan. 1978.

[8] A. V. Oppenheim and R. W. Schafer, *Discrete-Time Signal Processing.* Englewood Cliffs, NJ: Prentice-Hall, 1989.

[9] D. Slepian, H. J. Landau, and H. O. Pollak, “Prolate spheroidal wave functions, Fourier analysis, and uncertainty principle T and II,” *Bell Syst. Tech. J.,* vol. 40, no. 1, pp. 43–84, Jan. 1961.

[10] D. Slepian, “On bandwidth,” *Proc. IEEE,* vol. 64, pp. 292–300, Mar. 1976.

[11] G. Braileanu, “Matrix operators for numerically stable representation of stiff, linear dynamic systems,” *IEEE Trans. Automat. Contr.,* vol. 35, pp. 974–980, Aug. 1990.

[12] M. J. D. Powell, *Approximation Theory and Methods.* London, U.K.: Cambridge Univ. Press, 1981.

[13] W. H. Press, B. P. Flanery, S. A. Teukolsky, and W. T. Vetterling, *Numerical Recipes: The Art of Scientific Computing.* London, U.K.: Cambridge Univ. Press, 1986.

[14] T. I. Laakso, V. Välimäki, M. Karjalainen, and U. K. Laine, “Splitting the unit delay,” *IEEE Signal Processing Mag.,* vol. 13, pp. 30–60, Jan. 1996.

Cross-Coupled DOA Trackers

Ana Pérez-Neira, Miguel A. Lagunas, and R. Lynn Kirlin

***Abstract*— A new robust, low complexity algorithm for multiuser tracking is proposed, modifying the two-stage parallel architecture of the estimate-maximize (EM) algorithm. The algorithm copes with spatially colored noise, large differences in source powers, multipath, and crossing trajectories. Following a discussion on stability, the simulations demonstrate an asymptotic and tracking behavior that neither the EM nor a nonparallelized tracker can emulate.**

***Index Terms*— Array processing, DOA tracking, EM algorithm, extended Kalman filter, signal vector decoupling, space diversity.**

I. Introduction

Computational efficiency is a paramount issue in applying array signal processing to modern communications, and any objective or architecture will be of use only if there exists a feasibly implementable algorithm. The estimate-maximize (EM) algorithm [1], [2] stands out for reducing the computational complexity of the maximum likelihood (ML) estimation, while the Kalman filter [3], [4] provides a desirable linear solution to the complexity of spatially nonstationary scenarios. Our approach uniquely combines the EM two-stage parallel architecture of Feder and Weinstein [5] and Boheme *et al.* [2] with the adaptability of the Kalman filter.

We address a digital wireless communication system employing adaptive arrays for the localization of NS moving sources using an array of NQ identical radio receivers. The NS users operate simultaneously in the same bandwidth, and no restriction is imposed on the signals' cross correlations. The signal received by the qth sensor is a superposition of the NS source signals, having a time-varying delay $\tau_{kq}(n)$. Assuming that the signals are narrowband, the complex baseband signal $x_q(n)$ can be expressed as

$$x_q(n) = \sum_{k=1}^{\mathrm{NS}} e_k(n)\, \exp\left[jw_o \tau_{kq}(n)\right] + v_q(n) \tag{1}$$

where

$e_k(n)$ complex envelope representation of source k with respect to some fixed carrier frequency w_o;

Manuscript received April 18, 1996; revised April 18, 1997. This work was supported in part by the National Plans of Spain CICYT, Grants TIC92-08000-C05-05 and TIC96-0500-C10-01.

A. Pérez-Neira and M. A. Lagunas are with the Department of Signal Theory and Communications, Universitat Politécnica de Catalunya, Barcelona, Spain (e-mail: anuska@gps.tsc.upc.es).

R. L. Kirlin is with the Department of Electrical and Computer Engineering, University of Victoria, Victoria, B.C., Canada V8W 3P6 (e-mail: kirlin@sirius.uvic.ca).

Publisher Item Identifier S 1053-587X(97)07354-6.

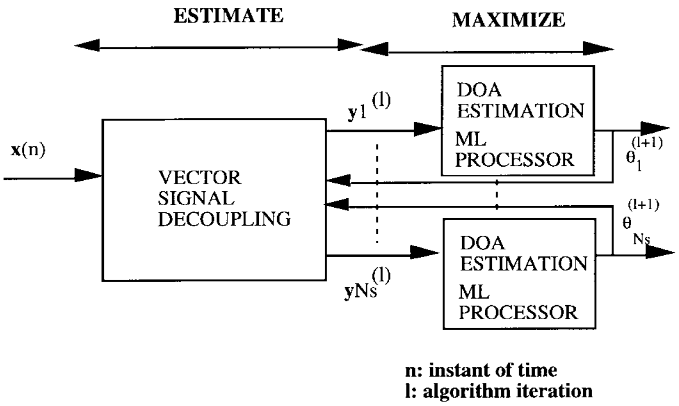

Fig. 1. Parallel architecture for DOA estimate via EM (DML estimate).

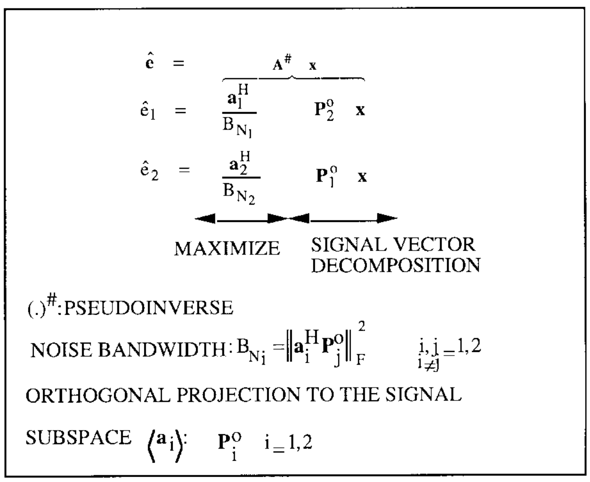

Fig. 2. Reformulation of the DML in a two-stage estimate (two-source case).

$v_q(n)$ Gaussian noise independent of the source signals and having covariance matrix $\mathbf{C}_v$.

In our work, a small number of snapshots is necessary to carry out an angle estimate (less than ten snapshots); thus, the relative array velocity does not change over the observation interval and can be assumed zero. Under this assumption and in the case of linear array, the delay ${}^{\tau}kq^{(n)}$ involves only the sensor location d_q and the source DOA θ_k relative to array broadside (for simplicity, we consider a linear array along the Y axis, although the work to be presented extends easily to planar arrays). The length NQ snapshot vector $\mathbf{x}(n)$ is given by

$$\mathbf{x}(n) = \mathbf{A}(n;\theta)\mathbf{e}(n) + \mathbf{v}(n) \tag{2}$$

where $\theta^T = [\theta_1 \cdots \theta_{Ns}]$ is the vector of source DOA's, and $\mathbf{e}(n)$ is composed of the NS complex emitter waveforms received at time n. Matrix $\mathbf{A}(n;\theta)$ is the NQ $\times$ NS steering matrix whose NS columns comprise the steering vectors $\mathbf{a}_k$, an element q of which (assuming perfect array calibration) is

$$[\mathbf{a}_k]_q = \exp\left[j\, 2\pi\, \frac{1}{\gamma}\, d_q\, \sin\theta_k(n)\right]. \tag{3}$$

The problem of interest is to estimate the NS sources' angular positions $\theta_k(n)$ using multiple $\mathbf{x}(n)$.

The EM algorithm (see Fig. 1), assuming an uncorrelated stationary source signal and noise process in a time invariant medium, iterates between the E-step and the M-step. The E-step uses the incomplete or observed data $\mathbf{x}$ and the current parameter estimate to estimate

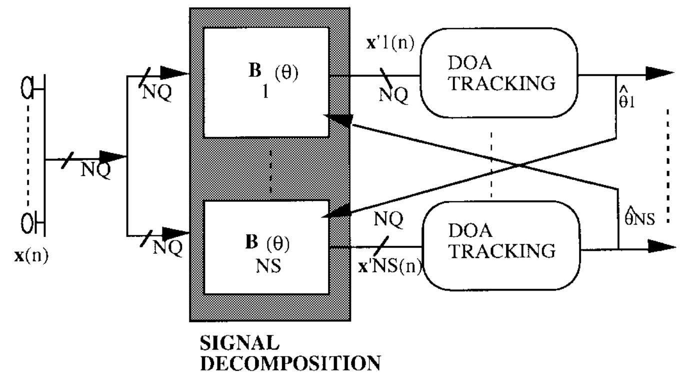

Fig. 3. DOA estimate feed-back in order to perform the signal decomposition.

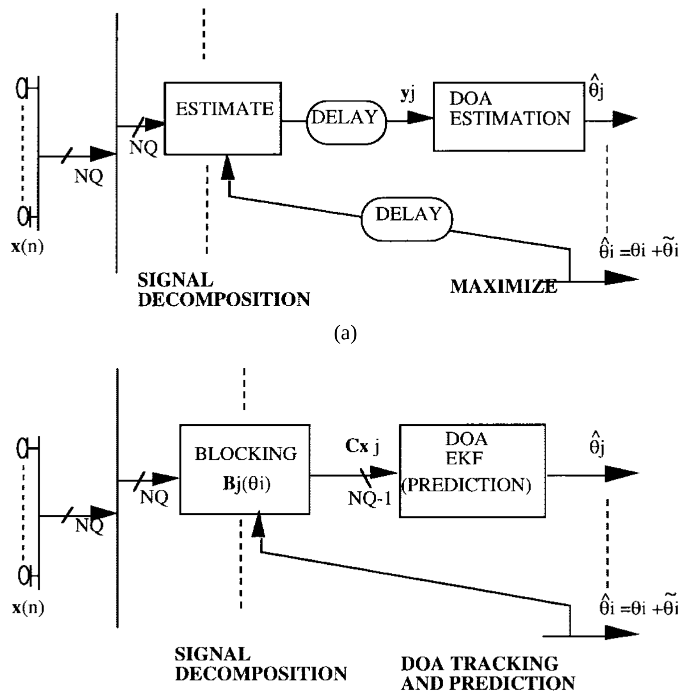

Fig. 4. Comparison of EM with the parallel system that is proposed in this work. Note that the EM has two delays in loop; system in (b) has one, therefore it is inherently more stable.

the log-likelihood of the complete data, producing decoupled signal vectors $\mathbf{y}_k$. The M-step then maximizes the estimated log-likelihood function and obtains a new DOA estimate. However, in a mobile context, all of the EM assumptions are not always valid. This motivates modification of the signal decoupling (Section II) and DOA estimation, respectively (Section III).

II. First Stage: Signal Vector Decoupling

This section replaces the source statistical diversity required by EM with spatial diversity (i.e., linear independence among the steering vectors) in order to decouple the signal vectors. In Fig. 2, it is seen that the ith projection matrix $\mathbf{P}_i^o(i = 1,\, 2)$ removes the contribution of source i from the data $\mathbf{x}$ and produces decoupled signal vectors $\mathbf{P}_i^o\mathbf{x}$. Using the independence among the source steering vectors, the deterministic maximum likelihood (DML) spatially filters the interfering sources. The authors propose in [6] a low complexity

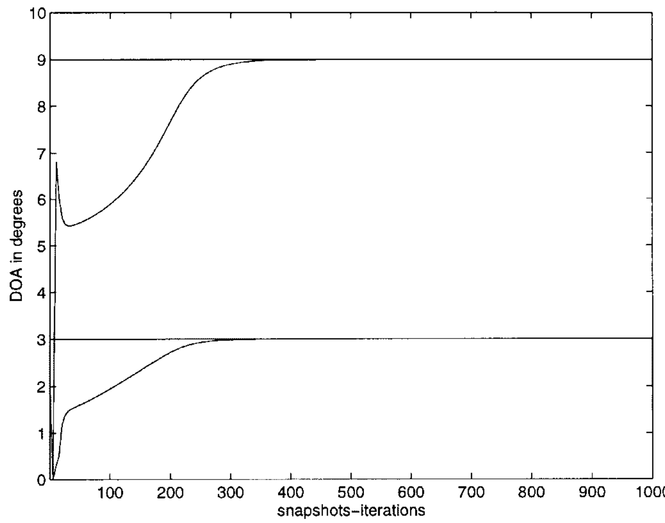

(a)

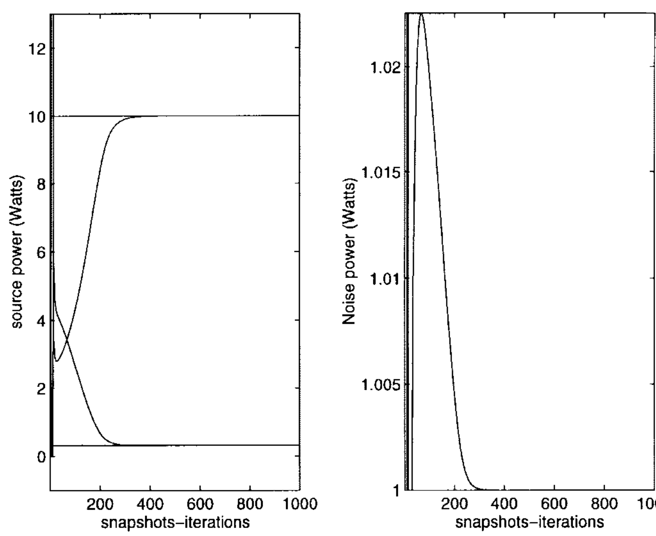

(b)

Fig. 5. Simulation with an exact data covariance matrix (EKF). Two sources at 9° and 3°, SNR $= [10 \quad -5]$ dB, noise power $= 0$ dB. (a) DOA estimate. (b) Source and noise power estimate.

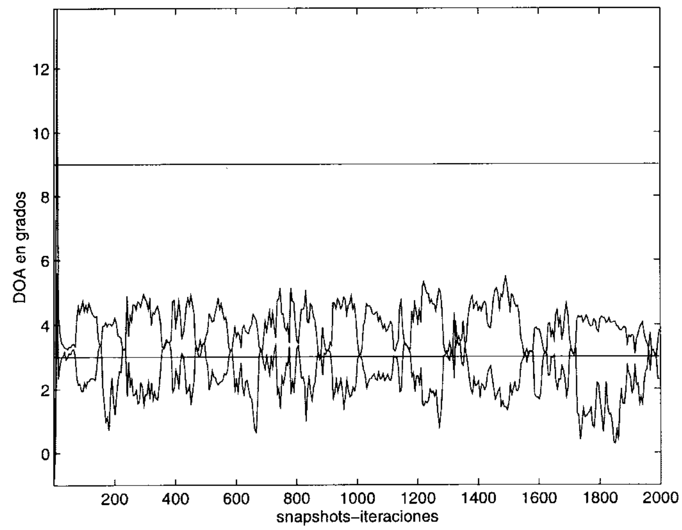

(a)

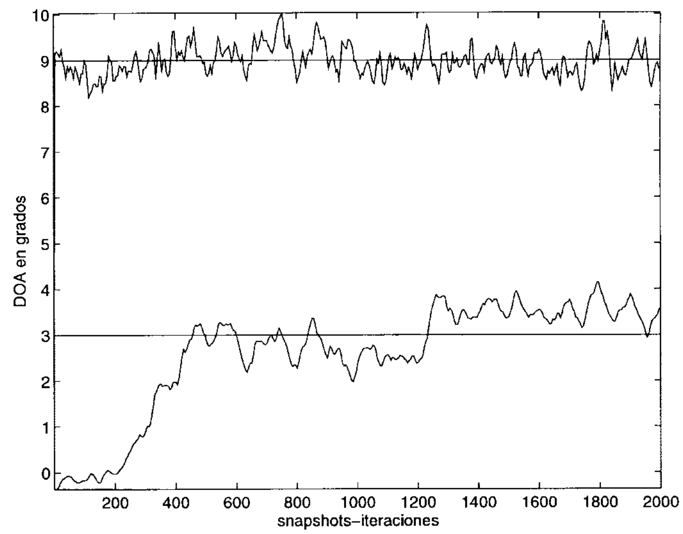

(b)

Fig. 6. Two BPSK sources of SNR $= [205]$ dB at 9° and 3°, respectively. (a) Seven sensor array. One single EKF (EKF). (b) Two parallel EKF (EKF_P) with blocking initialization at $1°$ and $-1°$.

spatial filtering alternative inspired in the work of Griffiths and Jim [7] and present an easy design that does not require EVD [8]. The blocking matrix for the case of a linear array and $j = 1 \cdots$ NS is

$$\mathbf{B}_j = \begin{bmatrix} 1 & -b_{j1} & 0 & \cdots & \cdots & 0 \\ 0 & 1 & -b_{j2} & 0 & \cdots & 0 \\ \cdots & \cdots & \cdots & \cdots & \cdots & \cdots \\ 0 & 0 & 0 & \cdots & 1 & -b_{j\mathrm{NQ}-1} \end{bmatrix} \tag{4a}$$

$$bjq = \exp\left[\frac{-j2\pi f}{c}\,(d_q - d_{q+1})\,\sin\theta_j\right]. \tag{4b}$$

We note the simplicity of the phase-only control and that feedback is necessary for neither signal waveform nor statistics. The proposed blocking matrix avoids both the stationarity and statistical independence requirements of EM. Additionally, even sources with very different powers will be decoupled; thus, the so-called near–far problem is avoided.

III. Second Stage: DOA Tracking

As Fig. 3 depicts, the second stage entails NS parallel processors, each one devoted to the estimation of a single source DOA. In contrast to the M-step in the EM, the emitted signals can be nonstationary, and in contrast to other Kalman applications in passive arrays [3], [9]–[12], our work introduces a novel extended Kalman filter (EKF) that estimates a portion of the data correlation matrix

$$\mathbf{C}_x = E\{\mathbf{x}\mathbf{x}^H\} = \mathbf{C}_s + \mathbf{C}_v \tag{5}$$

where $\mathbf{C}_v$ is the correlation of the data noise $v(n)$, and $\mathbf{C}_s$ is the source signal correlation matrix. We propose a computationally efficient error measure suitable for other than spatially white Gaussian noise; it uses only the first column of the error correlation matrix; thus, we have the vector quantity

$$\mathbf{r} = [\hat{\mathbf{C}}_x - \hat{\mathbf{C}}_s][1\,0\cdots 0]^T = [\hat{\mathbf{C}}x - \hat{\mathbf{C}}_s]\mathbf{1}. \tag{6}$$

The EKF estimates the parameter vector

$$\gamma = [\alpha \quad \theta]^T \tag{7}$$

where α and θ are the single-source power and DOA, respectively, as simulations show that noise power can also be included in the

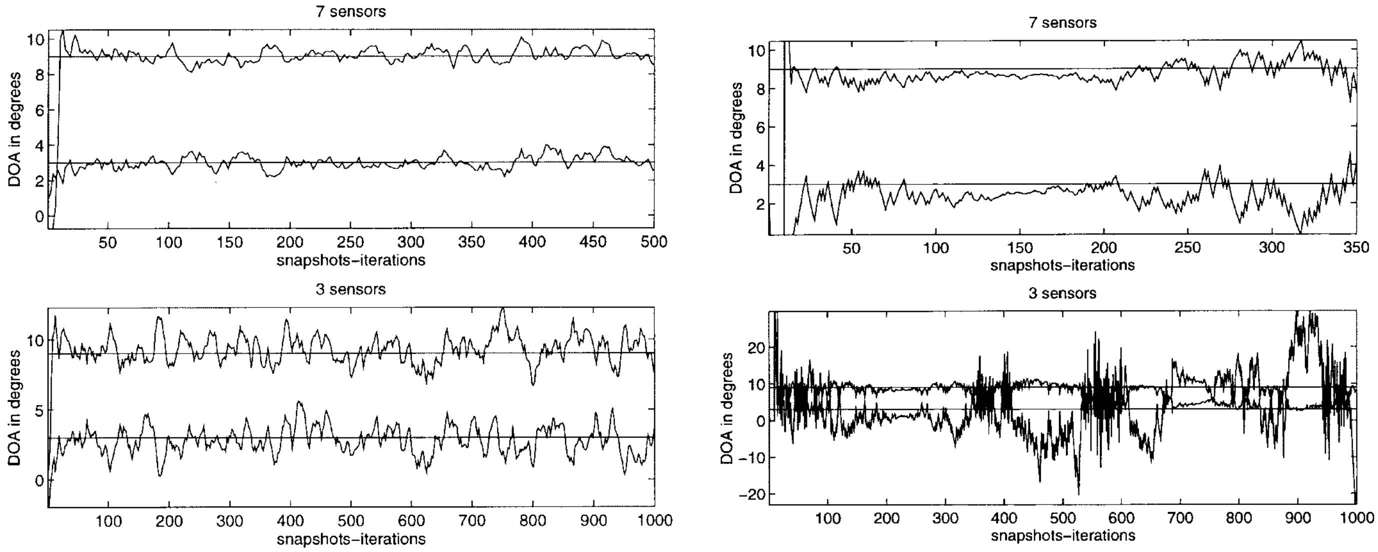

(a) (b)

Fig. 7. Two sources of 20 dB at 9° and 3°, respectively. (a) DOA estimate with EKF_P. (b) DOA estimate with EKF.

TABLE I

TWO EKF'S IN PARALLEL (EKF_P) ESTIMATING EACH ONE A DIFFERENT SOURCE DOA. ASYMPTOTIC RESULTS FOR THE DOA ESTIMATES AND ERROR PARAMETER CORRELATION ARE SHOWN (EKF RESULTS SHOWN IN PARENTHESES), 20 MONTE CARLO RUNS. TWO SOURCES AT 3° AND 9° OF EQUAL SNR. DOA INITIALIZED AT $-1°$ AND 1°. SOURCE AND NOISE POWER RANDOMLY INITIALIZED. INITIAL DATA COVARIANCE $\mathbf{C}_{xo} = 0$. COVARIANCE MATRICES IN EKF'S $\mathbf{R} = \mathbf{I}$, $\mathbf{Q} = 10^{-6}$, $\Sigma_{o/o} = 10^3$

		ESTIMATION IN BRANCH 1			ESTIMATION IN BRANCH 2		
SNR (dB)	N (samples)	DOA 1 bias	DOA 1 standard deviation	Parameter error correlation (from Σ1) x10^{-4}	Parameter error correlation (from Σ2) x10^{-4}	DOA 2 bias	DOA 2 standard deviation
5	500	0.62 (-0.02)	0.72 (0.85)	2,76 (0,26 < 2,76+ 0,38)	0,38	-1,11 (0,46)	1,17 (0,95)
	2000	-0,4 (0,07)	0,63 (0,78)	1,5 (0,23 < 1,5+ 1,3)	1,3	0,1 (0,05)	1,3 (0,55)
	5000	-0,33 (0,07)	0,54 (0,78)	1,3 (0,23 < 1,3+ 1,3)	1,3	-0,13 (-0,02)	0,48 (0,54)
10	500	0,37	0,59	0,62	0,15	-0,66	0,8
	2000	-0,2	0,58	0,44	0,4	-0,18	0,8
	5000	-0,2	0,52	0,38	0,4	-0,1	0,51
15	500	0,29	0,57	0,16	0,08	-0,13	0,59
	2000	-0,13	0,48	0,13	0,13	-0,17	0,53
	5000	-0,1	0,43	0,12	0,13	-0,07	0,44

parameter vector. The measurement error can be linearly modeled on the parameter error vector $\tilde{\gamma}$ as

$$\mathbf{r}_n \cong \varepsilon = \mathbf{H}^H \tilde{\gamma} + \mathbf{u} \tag{8a}$$

$$\mathbf{H} = [\mathbf{a}(\theta) \quad \mathbf{d}(\theta)] \tag{8b}$$

$$\mathbf{d}(\theta) = j\frac{2\pi f}{c}\, dq \operatorname{Cos}(\hat{\theta}_i)\, \mathbf{a}(\hat{\theta}). \tag{8c}$$

The vector $\mathbf{u}$, which is a bias term that includes possible model imperfections, has correlation matrix $\mathbf{R}$. If the structure of the data Gaussian noise covariance matrix $\mathbf{C}_v$ is known, γ may incorporate its parameters, and spatially colored noise may be reflected in the observation matrix $\mathbf{H}$.

Equation (8) and the *state or parameter model*

$$\gamma_{n+1} = \mathbf{F}_n\, \gamma_n + \mathbf{w}_n \tag{9}$$

constitute the basis of the proposed EKF. We note that the introduction of some kinematic parameters (i.e., speed, acceleration, etc.) in the parameter model improves the tracking performance and overcomes some of the problems of the crossing targets. The *updates* of the parameter estimates are

$$\hat{\gamma}_{n/n} = \hat{\gamma}_{n/n-1} + \mathbf{K}_n\, \varepsilon_n \tag{10}$$

where $\hat{\gamma}_{n/n-1}$ is the parameter vector estimated at time n with measurements up to instant $n-1$, and the optimum gain matrix is

$$\mathbf{K}_n = \textstyle\sum_{n/n-1} \mathbf{H}_n \left(\mathbf{H}_n^H \sum_{n/n-1} \mathbf{H}_n + \mathbf{R}_n\right)^{-1} \tag{11}$$

where $\sum_{n/n-1}$ is defined as the parameter error correlation matrix that is given recursively by the discrete-time Riccati equation [4].

All these equations simplify the computation whenever the parameter vector dimension is significantly smaller than the input data

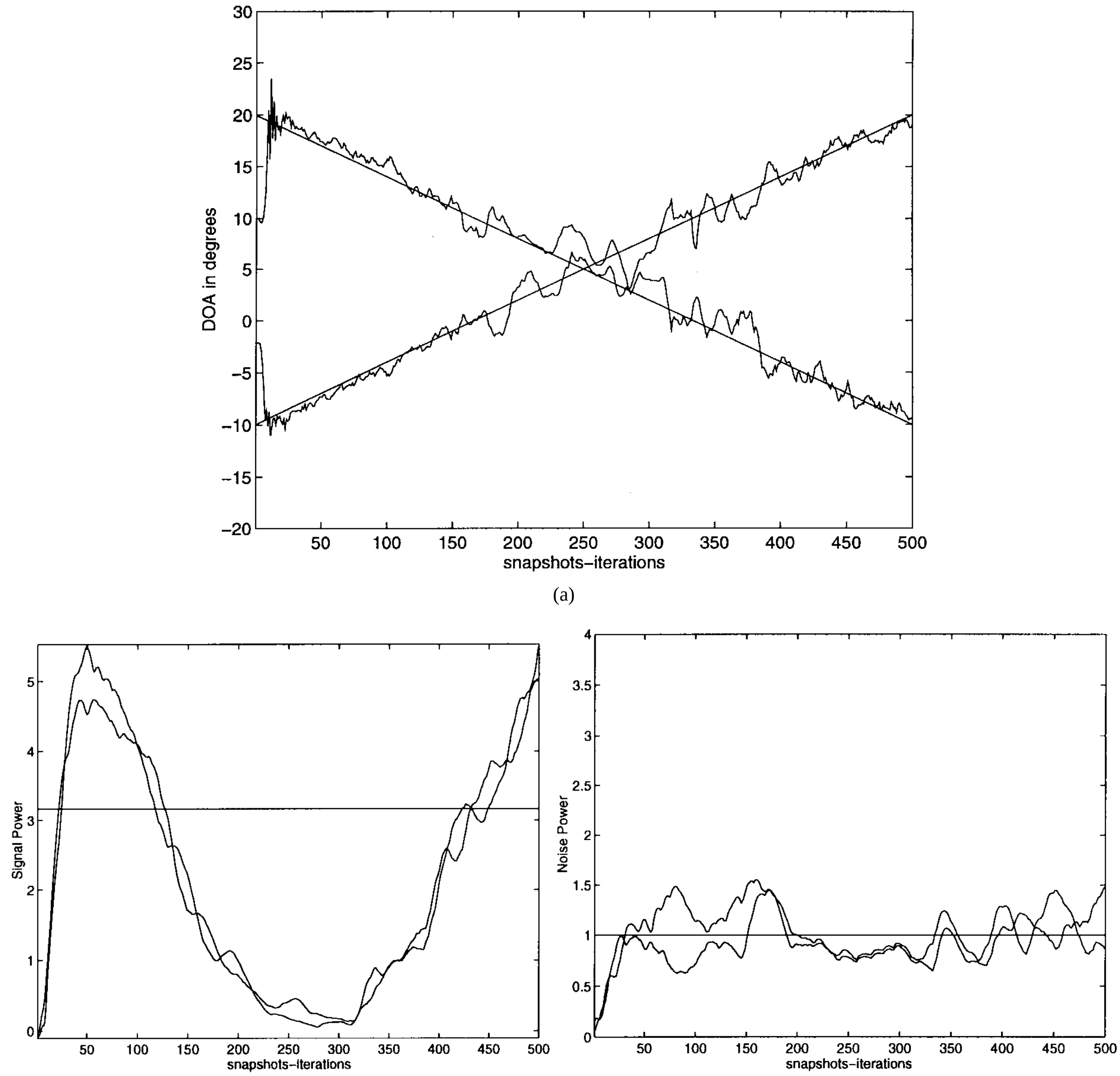

(a)

(b) (c)

Fig. 8. Scenario with two moving sources and two parallel EKF's (EKF_P), seven sensors, full coherent sources of 5 dB each, noise power $= 0$ dB, and model of the colored noise is introduced at each EKF. (a) DOA. (b) Signal power. (c) Estimated noise power evolution at each parallel EKF (actual noise power is equal to 1).

vector dimension [4, ch. 6]. The next section combines the designs in Sections II and III to produce the desired multisource tracker.

IV. Cross-Coupled DOA Trackers

The stability of the proposed system is essentially that of EM. For simplicity only, DOA is taken into account in the state vector of (7). As Fig. 4 depicts, if we feed the DOA angle error $\tilde{\theta}_i$ back into branch j via the blocking matrix $\mathbf{B}_j$, then an error in the covariance matrix $\mathbf{C}_{xj}$ (measurements) results. The gain from the DOA angle error to covariance matrix $\mathbf{C}_{xj}$ error β is found by taking the partial of b_{jq} in (4b) with respect to DOA angle. This results in a bias

$$\beta = \alpha_j(-j\,\pi\,\cos\theta_i)\,\mathbf{a}(\theta_j)\,\tilde{\theta}_i \tag{12}$$

which can be included in vector $\mathbf{u}$ [see (8a)]. This bias will not cause instabilities in the update equation (10) as long as the gain $\mathbf{K} < 1$; thus, the bias term can be counteracted and stability assured by augmenting the noise covariance matrix $\mathbf{R}_n$. Divergence occurs if the design error correlation $\mathbf{\Sigma}$ in (11) remains bounded while the error performance matrix [4, ch. 6], in fact, is unbounded or becomes very large relative to $\mathbf{\Sigma}$. For a qualitative stability study, we perform the simulations in the following section.

V. Simulations

We perform two sets or experiments under the following conditions. The base station has a perfectly calibrated linear uniform array of seven sensors with intersensor distance $\lambda/2$. The parameter vector consists of the DOA, source power, and noise power. We simulate only two users simultaneously demanding the space diversity multiple access (SDMA) because the probability of more than two is very low. The noise power is equal to 0 dB, $\hat{\mathbf{C}}_x$ has been estimated with a sliding window of constant $\beta = 0.9$, and the sources emit narrowband binary phase shift keyed (BPSK) signals. Sampling is at twice the receiver intermediate frequency of 500 kHz.

Experiment 1: Two tracking system implementations are simulated: "EKF_P" uses distinct, parallel single source trackers, whereas "EKF" tracks all the sources with a single estimation vector. The two sources are located at 3° and 9°, which is a separation less than the resolution of the seven sensor array.

- *Error covariance model:* Fig. 5 validates the capability of the EKF when the exact covariance matrix is known; the estimation of the DOA's, signal, and noise powers are perfect.
- *Steady-state performance and stability:* In Table I, the numbers without parentheses correspond to EKF_P, whereas the numbers in parentheses correspond to EKF. We note from Table I that for EKF_P, the DOA error correlation $\mathbf{\Sigma}$ for each branch is always less than unity because $\mathbf{R} = \mathbf{I}$; hence, stability is assured in the coupled loops. Thus, for a fixed SNR, the bias, variance, and the entries of the parameter correlation matrix $\mathbf{\Sigma}$ are almost invariant along the 5000 samples. Additionally, by summing appropriate entries in matrices Σ_1 and Σ_2, we verify that the summed correlation error of cross-coupled EKF (EKF-P) is always greater than that of the nonparallel EKF. As commented on in Section IV, this fact indicates that the parallel architecture is a more conservative filter design than the nonparallel one, which does not present instabilities due to feedback and blocking.
- *Advantages of the parallelization:* Fig. 6 illustrates a scenario of two BPSK signals received with very different power, and here, EKF_P clearly outperforms EKF. In Fig. 6(a), both DOA estimates of EKF collapse to that of the most powerful signal. In contrast, in Fig. 6(b), the power of the sources does not play any role in the blocking matrix of EKF_P, and the two sources are correctly decoupled.

Last, computational complexity is reduced in the EKF_P scheme by taking advantage of the source decoupling. As shown in Fig. 7(a), once the signals are decoupled with a seven-sensor resolution blocking, each parallel EKF can perform the DOA estimation with just three sensors. Although the estimation variance increases, the results are far better than those obtained with a single EKF (EKF) and three sensors [Fig. 7(b)]. We also point out the system's high resolution and fast convergence.

Experiment 2: Fig. 8 depicts the tracking behavior of our proposed system with an example having fully coherent sources moving at a high angular rate. The worst performance occurs when the source angles converge. We stress that in this tracking simulation, no specific trajectory model has been assumed for the sources [$\mathbf{F} = \mathbf{I}$ in (9)], thus exemplifying the robust behavior of the proposed system. It can be observed in Fig. 8(b) that, due to the spatial filtering in the decoupling stage, the source power at the input of each EKF decreases when the sources converge spatially.

VI. Conclusions

The proposed system can be viewed as a synthesis of the best features of EM and Kalman tracking, producing a novel although suboptimal design requiring only coarse DOA initialization. The system is able to track multiple correlated (i.e., multipath) source DOA's having crossing trajectories and considerably different powers (i.e., near-far problem) and in spatially colored noise. The parallel EKF's are robust with respect to poor DOA initialization due to the fact that the blocking causes a competition among the parallel branches and the EKF's search randomly for a source signal to lock on, behaving much as a random communication access system. The resulting low complexity system is highly practical in developing land mobile, satellite, and personal wireless communication systems. The simulations have qualitatively verified the performance and robustness of the two-stage competitive structure.

References

[1] A. P. Dempster *et al.*, "Maximum likelihood from incomplete data via the EM algorithm," *Ann. Roy. Stat. Soc.*, pp. 1–38, Dec. 1977.

[2] D. Kraus, D. Maiwald, and J. F. Böhme, "Maximum likelihood source location estimation via EM algorithm," in *Signal Processing VI: Theories and Applications.* New York: Elsevier, 1992, pp. 649–652.

[3] *Kalman Filtering: Theory and Applications*, H. W. Sorenson, Ed. New York: IEEE, 1985.

[4] B. Anderson and J. Moore, *Optimal Filtering, Information and System Science Series*, T. Kailath, Ed. Englewood Cliffs, NJ: Prentice-Hall, 1979.

[5] M. Feder and E. Weinstein, "Parameter estimation of superimposed signals using the EM algorithm," *IEEE Trans. Acoust., Speech, Signal Processing*, vol. 36, pp. 477–489, Apr. 1988.

[6] M. Najar, M. A. Lagunas, and A. Perez-Neira, "Source separation based on coupled single DOA estimation processors," in *Proc. ICASSP'93*, Minneapolis, Apr. 1993, pp. 336-339.

[7] L. J. Griffiths and C. W. Jim, "An alternative approach to linearly constrained adaptive beamforming," *IEEE Trans. Antennas Propagat.*, vol. AP-30, pp. 27–34, Jan. 1982.

[8] B. D. Van Veen, "Eigenstructure based partially adaptive array design," *IEEE Trans. Antennas Propagat.*, vol. 36, pp. 357–362, Mar. 1988.

[9] C. R. Rao, C. R. Sastry, and B. Zhou, "Tracking the DOA of multiple moving targets," *IEEE Trans. Signal Processing*, vol. 42, pp. 1133–1144, May 1994.

[10] C. Chang and J. Tabaczynski, "Application of state estimation to target tracking," *IEEE Trans. Automat. Contr.*, vol. AC-29, pp. 98–109, Feb. 1984.

[11] Y. Chen and C. Chiang, "Kalman-based estimator for DOA estimations," *IEEE Trans. Signal Processing*, vol. 42, pp. 3543–3547, Dec. 1994.

[12] Z. Raida, "Steering and adaptive antenna array by the simplified Kalman filter," *IEEE Trans. Antennas Propagat.*, vol. 43, pp. 627–629, June 1995.